

# Hybrid CO<sub>2</sub> based thermo-mechanical underground energy storage - a numerical geomechanical review

Daniel Bücken

Ruhr-University Bochum, Working Group 'Engineering Geology and Rock Mass Mechanics', Bochum, Germany; geomecon GmbH, Berlin, Germany

Tobias Backers

Ruhr-University Bochum, Working Group 'Engineering Geology and Rock Mass Mechanics', Bochum, Germany

**ABSTRACT:** The energy transition requires new ways of effectively and safely generating and storing energy. Multi-fluid geothermal energy systems, such as flexible CO<sub>2</sub> plume geothermal systems and porous medium compressed air energy storage can provide dependable baseload, dispatchable power to complement intermittent renewable energy sources, and underground energy storage capacities. Here, a supercharged hybrid gas-based energy storage (SH-GES) approach using CO<sub>2</sub> to store pressure and temperature is analyzed from a geomechanical perspective. This is crucial for safe storage operations. Using fully coupled multiphase THM simulations, a generic fault-bound reservoir model is used to evaluate the effect of cyclic storage operations and variable injection temperatures on stress alterations in and around the reservoirs, shifts in seal integrity, and fault stability. The preliminary findings suggest that employing SH-GES for energy storage is a viable option. However, additional research is needed to gather more data regarding the geomechanical impacts and storage efficiency.

*Keywords: energy storage, compressed gas, THM simulation, geomechanics.*

## 1 INTRODUCTION

The energy landscape is rapidly changing to mitigate the impact of climate change. The transition from traditional fossil energy sources to sustainable energy sources requires new energy systems, involving production and storage, to complement methods already in place. Most renewable energy sources produce energy intermittently, and not necessarily when needed. This leads to daily to seasonal discrepancies in energy consumption and production. Safe and efficient means of energy storage and baseload production are, hence, of growing importance. The subsurface can offer solutions to these challenges. Storage and extraction of energy by gaseous fluids in the subsurface are at the core of this study; it analyzes a supercharged hybrid gas-based energy storage (SH-GES) approach, using CO<sub>2</sub> to store pressure (i.e., mechanical energy) and temperature (i.e., heat energy), from a geomechanical perspective.

Numerous studies analyze CO<sub>2</sub>-based systems such as CO<sub>2</sub> plume geothermal (CPG, e.g., Brown 2000, Randolph & Saar 2011, Buscheck et al. 2014) systems and flexible CPG (CPG-F; Fleming et

al. 2022, Van Brummen et al. 2022) systems. These systems can provide dependable baseload, dispatchable power to complement intermittent renewable energy sources, and underground energy storage capacities. CO<sub>2</sub>-based systems can offer many benefits over water-based approaches, such as higher thermal extraction rates and thus the exploration of shallower plays compared to traditional geothermal systems. These approaches mainly focus on thermal energy storage.

Compressed air energy storage in geological porous formations (PM-CAES; Gasanzade et al., 2023) represents a different approach to balance out fluctuations of renewable energy production (Mouli-Castillo et al. 2019, Gasanzade et al. 2021). Compared to traditional salt cavern storage, much larger amounts of energy can be stored in porous formations. This approach mainly focuses on mechanical energy storage.

The SH-GES approach combines mechanical and thermal energy to effectively and flexibly produce and store energy. Subsurface setup and operational phases are shown in Figure 1. A fault-bound reservoir is chosen to assess a variety of geomechanical effects. Two porous reservoirs bound by impermeable formations are targeted: a lower reservoir in which the supercharged, i.e., heated and compressed gas is stored, and an upper reservoir storing the gas after cooling and decompression in the surface facilities. Initially, the two reservoirs are filled with cushion gas. During subsequent phase 1, surplus grid energy is used to thermally supercharge working gas from the upper reservoir and/or surface sources, compress it and inject it into the lower reservoir. Pressure in the upper reservoir will decrease, and pressure and temperature in the lower reservoir will increase. During phase 2 the stored gas is returned to the surface, where it is expanded and cooled to produce electricity and heat which can be fed into the respective grid. After energy extraction, the gas is injected into the upper reservoir. Pressure in the lower reservoir will drop, pressure in the upper reservoir will increase, and temperature in the upper reservoir will increase or decrease depending on the injection and energy extraction schemes. Phases 1 and 2 are flexibly alternating depending on energy availability and demand. The double-reservoir approach ensures a constant containment of the working gas, which is not released into the atmosphere after phase 1, but continuously stored.

This study numerically investigates the effects of the complex reservoir operations on the subsurface system using fully coupled thermo-hydro-mechanical simulations. Temperature and pressure changes as well as cyclic loading and unloading of the reservoir are considered. A generic reservoir model is used to evaluate stress alterations in and around the reservoirs and resulting alterations of seal integrity and fault stability. Energy production, grid and powerplant considerations, and process engineering issues are beyond the scope of this preliminary study.

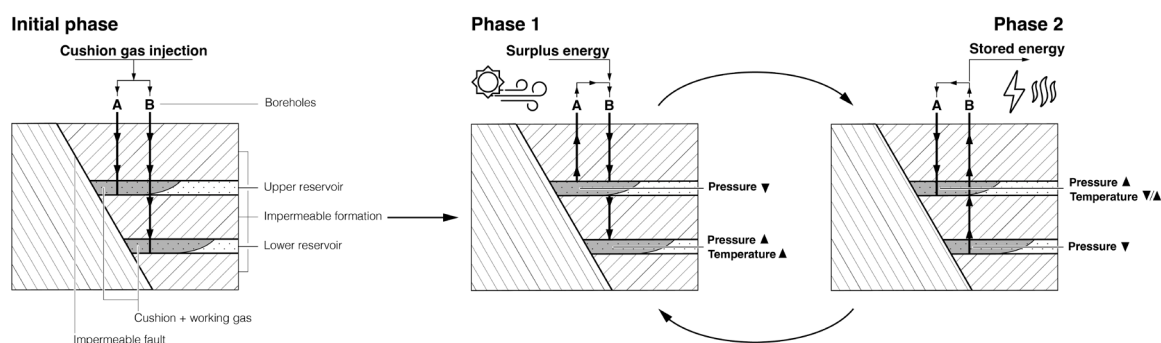


Figure 1. Setup and operational phases of the SH-GES approach.

## 2 NUMERICAL SIMULATION

The numerical simulations are carried out in the commercial finite element method code COMSOL Multiphysics. The underground model (Figure 2) consists of a  $25 \times 16$  km (E-W  $\times$  N-S) wide block of 5 km height, divided into a hanging wall and a footwall block separated by a fault plane oriented 180/75. The footwall block is homogeneous. The hanging wall block contains two 100 m thick reservoir units surrounded by uniform confining units. The reservoir tops are in 1,450 m and 2,450 m depth, respectively. The upper and lower reservoir are penetrated by borehole A and B,

respectively. The boreholes are placed 200 m from the fault plane relative to the borehole end, and only implemented inside the reservoirs. The open hole section of both boreholes is 80 m long, the 10 m at the top and bottom of the reservoir are not used for pumping operations. The model domain is discretized in more than 77,000 tetrahedral and hexagonal elements.

The two-phase flow in the reservoirs is modeled using the capillary pressure model of Brooks & Corey (1964) and Darcy's law. The pressure and temperature-dependent density and viscosity of CO<sub>2</sub> are computed using the Peng-Robinson (1976) equation of state and the Brokaw (1965) model with high-pressure viscosity correction. The rock mass is modeled using linear elasticity, coupled to subsurface flow via poroelasticity and to heat transfer via thermal expansion. The sides and bottom boundary of the model are constrained to plane-parallel movements only, the upper boundary is free. An external strike-slip stress field typical for Central Europe is applied (gradient vertical stress SV: 23 MPa/km, gradient minimum horizontal stress Sh: 18 MPa/km, gradient maximum horizontal stress SH: 25 MPa/km) with the direction of SH = 180°. The sides and bottom of the model are defined as no-flow boundaries and the top as an open boundary. The CO<sub>2</sub> concentration at the sides is fixed to zero. The initial conditions of the model are water filled with hydrostatic pore pressure and a geothermal gradient of 30 K/km with a ground-level temperature of 13°C. The petrophysical model parameters are given in Table 1. Confining units and footwall block share the same parameters. Dissolution of CO<sub>2</sub> into the pore water is not accounted for.

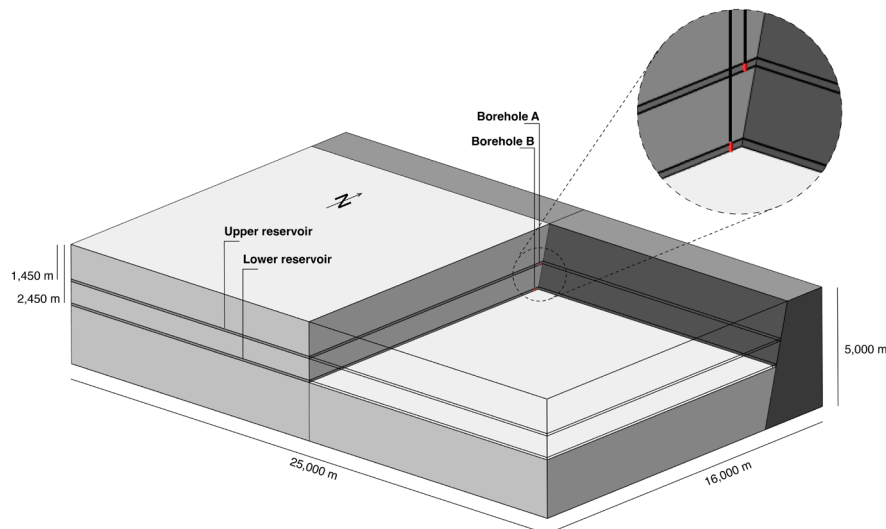


Figure 2. Subsurface model. Red borehole intervals represent the open-hole sections.

The numerical evaluation is carried out in two steps (Figure 3). An initial transient study simulates the injection of ca. 7.9E9 kg of CO<sub>2</sub> into the upper and the lower reservoir, respectively. Injection temperature is equal to the respective reservoir temperature. A second transient study consequently models the alternating injection and production from and into the upper and lower reservoir over the course of one year, respectively. The duration of one injection/production step (pump cycle from here on) is 90 days. The injection rate is 5 kg/s, while production is modeled as an open outflow, not a fixed production rate.

The spread between reservoir temperature and injection temperature ( $\Delta T$ ) was varied for both the upper and lower reservoir.  $\Delta T$  was -15 K, 0 K, and +15 K for the upper reservoir and 0 K, +20 K, and +50 K for the lower reservoir, resulting in a total of nine different injection temperature combinations, each modeled in a separate simulation.

The geomechanical parameters used to assess the reservoir integrity are the safety factor of the fault ( $SF_F$ ), defined as the friction coefficient of the fault (assumed as 0.4) divided by the ratio of acting shear and normal stress, and the safety factor of the reservoir ( $SF_R$ ), defined as the sinus of the friction angle of the reservoir (assumed as 0.65) divided by the ratio of the difference between maximum and minimum principal stress and the sum of maximum and minimum principal stress (based on Mohr-Coulomb failure of a most critical discontinuity). The critical value of the safety

factors is 1. Additionally, the stresses acting on the bedding planes are monitored to assess whether tensile stresses are affecting seal integrity.

Table 1. Petrophysical model parameters.

Parameter		Reservoir	Confining units / footwall block
Young's modulus	[GPa]		16
Poisson's ratio	[1]		0.28
Density	[kg/m <sup>3</sup> ]		2450
Friction coefficient	[1]	0.85	0.4*
Biot-Willis coefficient	[1]		1
Porosity	[1]	0.2	0.01
Permeability	[mD]	500	10E-4
Coefficient of thermal expansion	[K <sup>-1</sup> ]		6E-6
Capillary entry pressure	[Pa]	10E5	10E6
Pore size distribution index	[1]		2.5
Residual water saturation	[1]		0.3
Residual gas saturation	[1]		0.25

\*fault plane

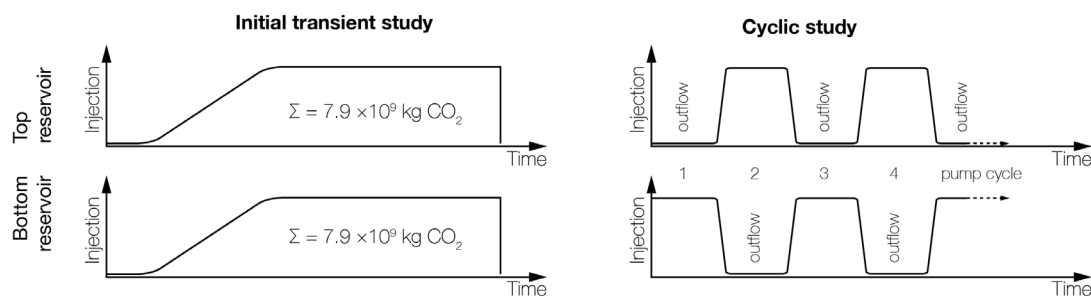


Figure 3. Numerical modeling steps, for upper and lower reservoir.

### 3 RESULTS

The fault plane remains stable in all simulations, with  $SF_F$  not falling below 6.9 (initial  $SF_F = 8.1$ ).  $SF_R$  remained uncritical in all simulations, too, with a minimum of 2.08 (initial  $SF_R = 2.12$ ) during the cyclic operations. Additionally, no tensile stresses were observed. Figure 4 displays the correlation matrix of the key parameters of all simulated scenarios. Maximum reservoir pressures (water and  $CO_2$ ) in the upper and lower reservoir have a strong negative correlation with the respective safety factors. The correlation between maximum and minimum reservoir temperature and safety factors is poor. Injection rates correlate negatively with the respective reservoir, and positively with the opposite reservoir.  $SF_F$  and  $SF_R$  for the respective reservoir correlate strongly and are not further distinguished in the following.

$SF_F$  for the upper reservoir ( $SF_{F\_up}$ ) is lowest for cycles 2 and 4 (injection in upper reservoir, outflow in lower reservoir, Figure 5).  $SF_{F\_up}$  has a positive correlation with the maximum temperature in the lower reservoir. Furthermore,  $SF_{F\_up}$  decreases with increasing reservoir pressure. The influence of the temperature spread appears minor. Similar trends can be observed for the  $SF_F$  in the upper reservoir ( $SF_{F\_lo}$ ), which increases with increasing temperatures in the upper reservoir and decreases with increasing pressures in the lower reservoir.

Reservoir temperatures generally increase up to 2.5 K during cushion gas injection. The temperature changes induced by the cyclic operations are spatially restricted to the near wellbore zone. Overall, the pressure and temperature of the lower reservoir are increasing with every injection cycle.

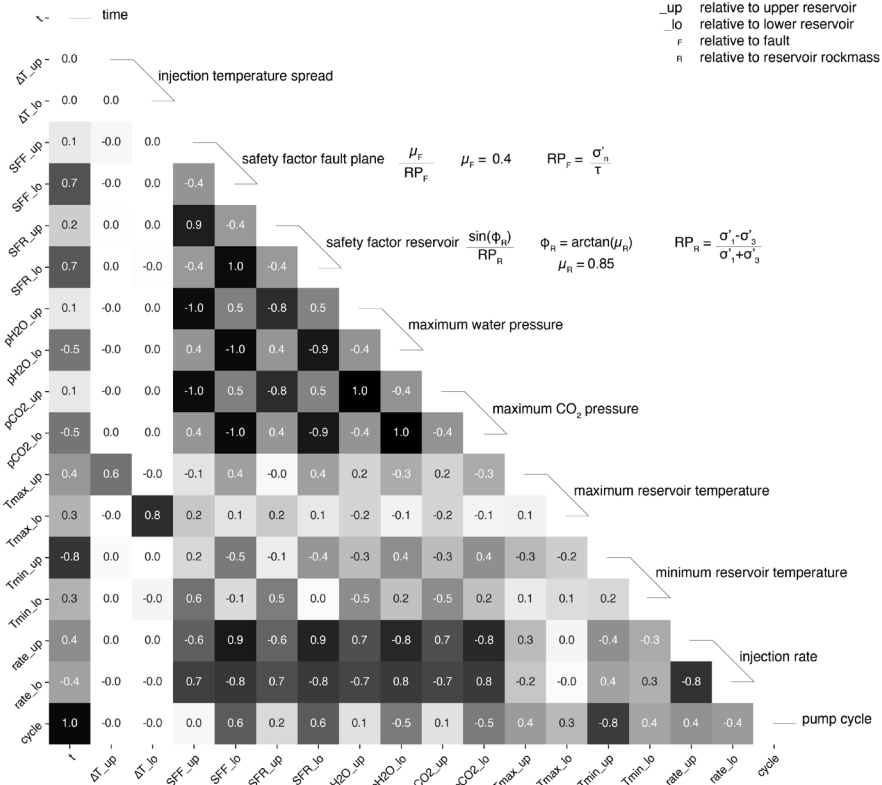


Figure 4. Pearson correlation coefficient for key parameters of all simulated scenarios.

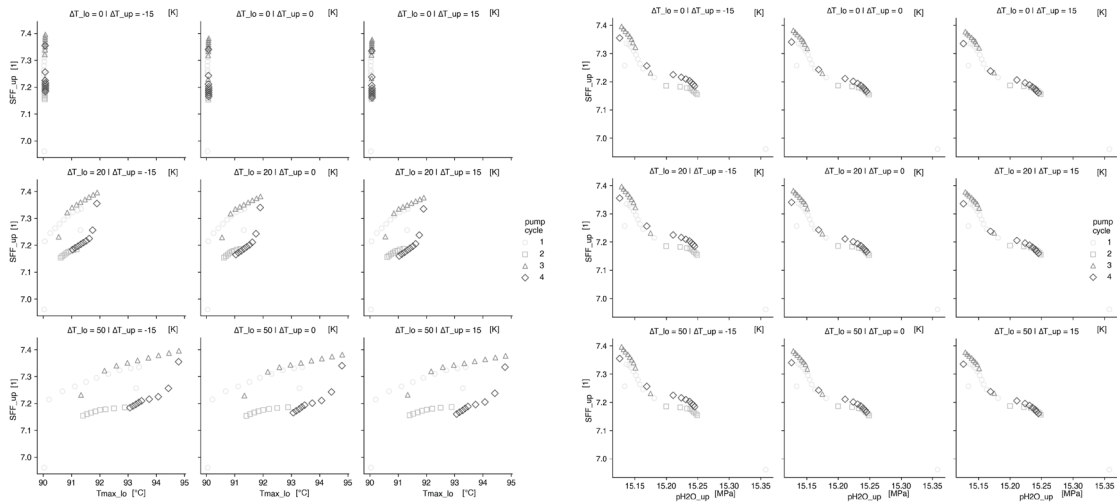


Figure 5. Left: scatter plots of maximal reservoir temperature (lower reservoir) vs  $SF_{F\_up}$  grouped by injection temperature spread, categorized by pump cycle. Right: scatter plots of maximal water pressure (upper reservoir) vs  $SF_{F\_up}$  grouped by injection temperature spread, categorized by pump cycle.

## 4 DISCUSSION

Reservoir integrity is not critically affected by the modeled scenarios. Increasing pressure destabilizes the respective reservoir, concordant with effective stress theory. Increasing temperatures appear to stabilize the opposite reservoir; this could however be caused by a pressure drop in the respective reservoir during these pump cycles. Cross-reservoir interaction is inconclusive. Temperature effects during cyclic operations are minor, as the pump cycles of 90 days only lead to

spatially confined temperature changes in the reservoir. Pressure effects are sensitive to injection rates, as the high mobility of CO<sub>2</sub> leads to swift pressure drops during outflow phases. Conversely, temperature changes are more sensitive to pump cycles, as they are not quickly compensated during outflow phases. Temperatures and pressures are stored over the injection cycles and can be retrieved during outflow phases. Storage efficiency should be further studied in following analyses.

We expect that longer pump cycles and longer overall simulation of storage operations lead to a stronger impact on reservoir integrity, possibly compromising the reservoirs. The effect of thermoelastic and poroelastic stress changes is expected to be stronger with longer pump cycles and storage operations. We recommend longer simulations to understand the complex interaction and the effect of these changes on reservoir integrity. Injection rates should be varied as we expect stronger effects from higher rates. The effect of changing model geometries and rock mass parameters should be assessed, as well as the usage of different cushion and working gasses.

## 5 CONCLUSION

We present a supercharged hybrid gas-based energy storage (SH-GES) approach using CO<sub>2</sub> to store pressure and temperature. We use fully coupled multiphase THM simulations to assess the geomechanical implications of safe storage operations. A generic fault-bound reservoir model is used to evaluate the effect of cyclic storage operations and variable injection temperatures on stress alterations in and around the reservoirs, shifts in seal integrity, and fault stability. This initial study indicates that energy storage using SH-GES is feasible. Further studies are advised to gather more information on geomechanical effects and storage efficiency.

## REFERENCES

- Brokaw, R. S. (1965). Approximate Formulas for the Viscosity and Thermal Conductivity of Gas Mixtures. II. *The Journal of Chemical Physics*, 42(4), 1140–1146.
- Brooks, R. H., & Corey, A. T. (1964). Hydraulic properties of porous media. Hydrology Paper No. 3. *Civil Engineering Department, Colorado State University, Fort Collins, CO*.
- Brown, D. W. (2000). A hot dry rock geothermal energy concept utilizing supercritical CO<sub>2</sub> instead of water. 233–238.
- Buscheck, T. A., Bielicki, J. M., Chen, M., Sun, Y., Hao, Y., Edmunds, T. A., Saar, M. O., & Randolph, J. B. (2014). Integrating CO<sub>2</sub> Storage with Geothermal Resources for Dispatchable Renewable Electricity. *Energy Procedia*, 63, 7619–7630.
- Fleming, M. R., Adams, B. M., Ogland-Hand, J. D., Bielicki, J. M., Kuehn, T. H., & Saar, M. O. (2022). Flexible CO<sub>2</sub>-plume geothermal (CPG-F): Using geologically stored CO<sub>2</sub> to provide dispatchable power and energy storage. *Energy Conversion and Management*, 253, 115082.
- Gasanzade, F., Pfeiffer, W. T., Witte, F., Tuschy, I., & Bauer, S. (2021). Subsurface renewable energy storage capacity for hydrogen, methane and compressed air – A performance assessment study from the North German Basin. *Renewable and Sustainable Energy Reviews*, 149, 111422.
- Gasanzade, F., Witte, F., Tuschy, I., & Bauer, S. (2023). Integration of geological compressed air energy storage into future energy supply systems dominated by renewable power sources. *Energy Conversion and Management*, 277, 116643.
- Mouli-Castillo, J., Wilkinson, M., Mignard, D., McDermott, C., Haszeldine, R. S., & Shipton, Z. K. (2019). Inter-seasonal compressed-air energy storage using saline aquifers. *Nature Energy*, 4(2), Article 2.
- Peng, D.-Y., & Robinson, D. B. (1976). A New Two-Constant Equation of State. *Industrial & Engineering Chemistry Fundamentals*, 15(1), 59–64.
- Randolph, J. B., & Saar, M. O. (2011). Coupling carbon dioxide sequestration with geothermal energy capture in naturally permeable, porous geologic formations: Implications for CO<sub>2</sub> sequestration. *Energy Procedia*, 4, 2206–2213.
- Van Brummen, A. C., Adams, B. M., Wu, R., Ogland-Hand, J. D., & Saar, M. O. (2022). Using CO<sub>2</sub>-Plume geothermal (CPG) energy technologies to support wind and solar power in renewable-heavy electricity systems. *Renewable and Sustainable Energy Transition*, 2, 100026.